# Top Leads for Swine Influenza A/H1N1 Virus Revealed by Steered Molecular Dynamics Approach

Binh Khanh Mai,[†] Man Hoang Viet,[‡] and Mai Suan Li*[,‡]

Institute for Computational Science and Technology, 6 Quarter, Linh Trung Ward, Thu Duc District, Ho Chi Minh City, Vietnam, and Institute of Physics, Polish Academy of Sciences, Al. Lotnikow 32/46, 02-668 Warsaw, Poland

Received September 3, 2010

Since March 2009, the rapid spread of infection during the recent A/H1N1 swine flu pandemic has raised concerns of a far more dangerous outcome should this virus become resistant to current drug therapies. Currently oseltamivir (tamiflu) is intensively used for the treatment of influenza and is reported effective for 2009 A/H1N1 virus. However, as this virus is evolving fast, some drug-resistant strains are emerging. Therefore, it is critical to seek alternative treatments and identify roots of the drug resistance. In this paper, we use the steered molecular dynamics (SMD) approach to estimate the binding affinity of ligands to the glycoprotein neuraminidase. Our idea is based on the hypothesis that the larger is the force needed to unbind a ligand from a receptor the higher its binding affinity. Using all-atom models with Gromos force field 43a1 and explicit water, we have studied the binding ability of 32 ligands to glycoprotein neuraminidase from swine flu virus A/H1N1. The electrostatic interaction is shown to play a more important role in binding affinity than the van der Waals one. We have found that four ligands 141562, 5069, 46080, and 117079 from the NSC set are the most promising candidates to cope with this virus, while peramivir, oseltamivir, and zanamivir are ranked **8**, **11**, and **20**. The observation that these four ligands are better than existing commercial drugs has been also confirmed by our results on the binding free energies obtained by the molecular mechanics−Poisson−Boltzmann surface area (MM-PBSA) method. Our prediction may be useful for the therapeutic application.

## INTRODUCTION

Influenza virus contains two glycoproteins hemagglutinin and neuraminidase (NA). Sixteen subtypes of hemagglutinin (H1−H16) and nine subtypes of neuraminidase (N1−N9) were identified.[1] Hemagglutinin can binds with sialic acid receptor on the surface of cell and supports the entry of influenza virus into the cell. After replication of virus in the cell, neuraminidase cleaves the linkage between sialic acid and virus, releasing new forms of virus from the infected cell.[2] Because neuraminidase plays the important role in release of progeny virus to healthy cells and its active site is quite well-conserved, it has become the target for designing drugs against influenza.[3]

Nowadays, swine influenza virus type A (A/H1N1) spreads all over the globe and causes deaths of infected people.[4,5] The analysis of A/H1N1 virus suggests that this new strain had been circulating in pigs for almost a decade and probably jumped to humans months before it was detected in Mexico in March 2009. Oseltamivir (tamiflu) is currently the frontline antiviral drug used to fight the flu virus by inhibiting neuraminidase, a flu protein responsible for the release of newly synthesized virons. The dangerousness of this pandemic is not only because of its high rate spread via human, like the avian flu A/H5N1,[6] but also strains of both the A/H5N1[7,8] and A/H1N1[9−11] influenza virus can resist to oseltamivir. Thus it becomes vital to design a drug which would be better than existing drugs for treatment of influenza.

This problem has motivated numerous computational studies. Using the structure-based screening, in addition to 5 existing ligands, Cheng et al.[12] have obtained the list of 27 ligands as top-hits for A/H5N1 (Materials and Methods). Ligand 109836 from the NSC database (see http://129.43.27.140/ncidb2/) was found to be the most promising lead[12] to cope with the avian flu. Applying Autodock tool 1.5.2,[13] Nguyen et al.[14] have examined the binding affinity of 32 ligands, taken from the work of Cheng et al.,[12] to the swine A/H1N1 neuraminidase (A/H1N1 NA). They have found that instead of NSC109836, NSC211332 is a champion lead for the swine influenza virus.

In term of CPU time, the docking approach,[12,15−22] where the dynamics of a receptor is ignored, is computationally less expensive but its prediction ability is limited. Using the Autodock method,[23] it was shown,[24] for example, that oseltamivir has almost the same binding affinity to the wild type (WT) and H274Y variant of H5N1 neuraminidase. This result contradicts the experiments[25] showing that oseltamivir binds to WT stronger. Other methods such as linear interaction energy,[26−28] free energy perturbation,[29,30] linear response approximation,[31,32] molecular mechanics−Poisson−Boltzmann surface area (MM-PBSA),[33−35] molecular mechanics−generalized Born surface area,[36] and thermodynamic integration[37] can provide more reliable information, but they are very CPU demanding as the computation of binding free energy requires good configurational sampling in all-atom molecular dynamics (MD) simulations. Recently, the steered molecular dynamics

* To whom correspondence should be addressed: E-mail: masli@ifpan.edu.pl.
† Institute for Computational Science and Technology.
‡ Institute of Physics.

10.1021/ci100346s 
Published on Web 11/23/2010

(SMD) method[38,39] has been developed and successfully applied to understand mechanical unfolding of biomolecules and the unbinding process of ligands from receptors.[40−45] The free energy and potential of mean force may be also calculated using SMD, the Jarzynski's equality,[46−48] and weighted histogram analysis method.[49,50] However, this approach is CPU demanding for such long protein as A/H1N1 NA because a large number of trajectories between ligand bound and unbound states should be generated to obtain reasonable estimations.

In this paper, we propose to screen out ligands that are possibly more suitable for treatment of A/H1N1 influenza than Tamiflu and zanamivir (Relenza) using the SMD method. Our simple idea is based on the hypothesis that the larger rupture force needed to pull out a ligand from a receptor, the higher is ligand binding ability with protein (or the lower is binding free energy). In other words, instead of calculating the binding free energy, we estimate the unbinding force defined as a maximum force $F_{max}$ on the force-time or force-displacement profile of a ligand.

To check validity of the SMD approach, we first consider unbinding of Tamiflu from the wild-type (WT) and four mutants of neuraminidase from H5N1.[25,33] We have made this choice because the binding free energies of these complexes have been determined not only by the experiments[25] but also by the all-atom simulations using the Amber99 force field[51] and the MM-PBSA method.[33] In many cases, the MM-PBSA method[52,53] has been successfully applied to estimate binding free energies between proteins and ligands as it provides good correlation with experimental values.[33,54−56] Having used the Gromos96 force field f43a1[57] and the SMD simulations with a constant velocity, we showed that $F_{max}$ of four strains of A/H5N1 neuraminidase (A/H5N1 NA) is strongly correlated with the corresponding binding free energies reported by the experimental[25] and theoretical groups.[33] This suggests that the SMD might be used to study the binding affinity of ligands to neuraminidase.

Applying the SMD to pull 32 ligands[12] from the swine A/H1N1 NA, we have demonstrated that peramivir, Tamiflu, and Relenza are ranked **8**, **11**, and **20**, respectively ($F_{max}$ has been used for ranking). Contrary to prior results,[12,14] four ligands 141562, 5069, 46080, and 117079 from the NSC set were found to be the most prominent for combating with the swine A/H1N1 virus. This results has been also confirmed by by our estimates of the binding free energies for these four ligands and the three FDA proved drugs (Tamiflu, Relenza, and peramivir) using the MM-PBSA approach. Our finding may be useful for therapeutic purposes. From the methodology point of view, it is important to stress that the SMD has been shown to have the same reliability as the standard MM-PBSA method in predicting binding affinity but is computationally much more efficient.

## MATERIALS AND METHODS

**Crystal Structures of WT and Mutants of A/H5N1 Neuraminidase Bound with Oseltamivir.** Coordinates for the WT A/H5N1 NA were taken from a Protein Data Bank (PDB ID 2HU0)[58] and were used as the starting conformation in our simulations. Because 2HU0 is a tetramer, we extract only chain B, which has tamiflu bound to neuraminidase. To test the SMD method, we have applied it to pull the tamiflu from the WT and mutants N294S, H274Y and E119G of A/H5N1 NA the binding free energies of which were estimated previously[33] by the MM-PBSA method. We have also considered the mutant Y252H because, together with WT, N294S, and H274Y, its binding free energy has been already determined experimentally.[25]

Coordinates of the mutants N294S and H274Y bound with tamiflu in the active site were taken from structures 3CL2 (monomer) and 3CL0 (monomer), respectively.[25] The mutants E119G and Y252H were created with the help of the Mutagenesis module (http://pymolwiki.org/index.php/Mutagenesis) implemented in the PYMOL package (http://pymol.sourceforge.net). This module allows one to replace a given residue by a different one.

**Molecular Model for the Swine A/H1N1 Neuraminidase.** The amino acid sequence of A/H1N1 NA was obtained from Genbank Locus IS CY041156, but its crystal structure has not been determined yet. The sequence alignment performed by the homology modeling module in Discovery Studio 2.0 software, showed that A/H1N1 NA has very high sequence identity (∼92%) with A/H5N1 NA.[59] Therefore, a homology model of A/H1N1 NA was built using A/H5N1 NA as a starting point and by mutating corresponding residues to match the A/H1N1 NA with the help of the mentioned above Mutagenesis module in the PYMOL package. At the active site, the notable different between A/H5N1 and A/H1N1 neuraminidases is the replacement of Tyr347 by Asn347.

**Set of Ligands.** We have chosen 27 top-hit compounds obtained for A/H5N1 by Cheng et al.[12] and five additional ligands including Tamiflu, Relenza, peramivir, SA (sialic acid), and DANA (2,3-didehydro-2-deoxy-*N*-acetyl neuraminic acid). Atomic types, charges and other parameters of ligands were assigned using parameters of the Gromos force field 43a1.[60] Hydrogen atoms are added by using the Dundee PRODRG2.5 Server (beta)[61] with the same force field. Ligands are put into the drug binding pocket by the autodock method.[13] Since positions of tamiflu in the active site of WT A/H5N1 NA and its mutants N294S and H274Y are known from PDB, to check the validity of this approach, we have used it to put tamiflu into the binding pocket of these systems. It turns out that positions of tamiflu in the active site obtained by the autodock are similar to those from PDB.

**Steered Molecular Dynamics (SMD).** The neuraminidase-ligand complexes were placed in a triclinic box with the edges of 7.25, 7, and 9 nm which contains approximately 13200 water molecules (Figure 1). The center of the protein is placed at 4, 3.9, and 3.25 nm. The protein is rotated in such a way that its binding site directs toward the pulling *z*-direction the definition of which is given in the main text (see also below). To neutralize systems $Na^+$ or $Cl^-$ counterions are added using the command "Genion" in the Gromacs suite (Figure 1).

The GROMACS 4.0.5 package[57] was used to run MD simulations with the GROMOS96 43a1 force field[60] and the SPC water model.[62] The equations of motion were integrated by using a leapfrog algorithm[63] with a time step of 2 fs. The LINCS algorithm[64] was used to constrain the length of all bonds. vdW forces were calculated with a cutoff of 1.4 nm, and particle-mesh Ewald method[65] was employed to treat the long-range electrostatic interactions. The nonbonded interaction pair-list was updated every 10 fs with the cutoff of 1 nm. After minimization by the steepest descent method,

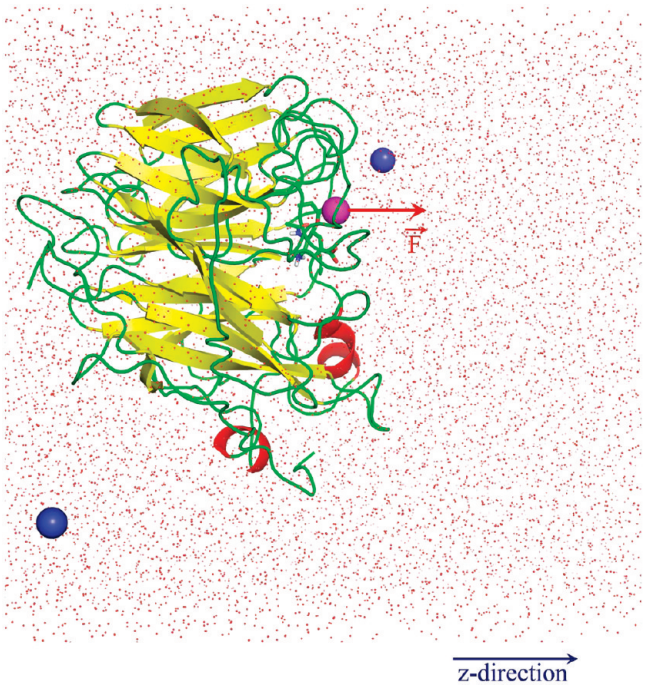


**Figure 1.** Initial structure for pulling tamiflu from A/H1N1 NA. The magenta ball (enlarged) refers to the atom to which the force is applied. Blue spheres are ions $Na^+$ added to neutralize the system.

position-restrained MD simulations were performed for 100 ps to let water molecules move into the active site. Then the whole system was gradually heated from 0 to 300 K during 500 ps of the MD run. To make sure that the complex is stable, the system was equilibrated for 500 ps at 300K in the NVT ensemble run with the Berendsen procedure[66] and, subsequently in 500 ps NPT ensemble run at pressure of 1 atm. The Parrinello−Rahman pressure coupling[67] has been used.

After equilibration, through a virtual cantilever moving at the constant velocity $v$ along the biggest $z$-axis of simulation box (see the choice of pulling direction below and in the main text), the force was applied to that atom of ligand which is closest to the outsite bound of the binding site in the $z$-direction (Figure 1). The spring constant was chosen as $k = 600$ kJ/(mol nm$^2$) $\approx 1020$ pN/nm which is a typical value for $k$ of cantilever used in atomic force microscopy experiments. Movement of the pulled ligand causes an rupture of hydrogen bonds (HBs) between it and protein, and the total force was measured by $F = k(vt - x)$, where $x$ is the displacement of the pulled atom from its original position.

We have tried pulling speeds $v = 0.005$ nm/ps and $v = 0.01$ nm/ps. Since results are essentially the same for both cases, we will present results obtained for $v = 0.005$ nm/ps. For this value of $v$, one needs to make SMD runs for 500−600 ps to entirely move the ligand out from the receptor. To ensure robustness of results, four independent trajectories were generated using different random number seeds.

**Choice of Pulling Path.** It is well-known from studies of mechanical unfolding of proteins, the rupture force is sensitive to pulling direction.[68−70] Therefore, it is important to establish what pulling path should be chosen. For this purpose, we probe pulling pathways of Tamiflu from the active site of WT A/H5N1 NA, using Caver 2.0,[71] a plugin

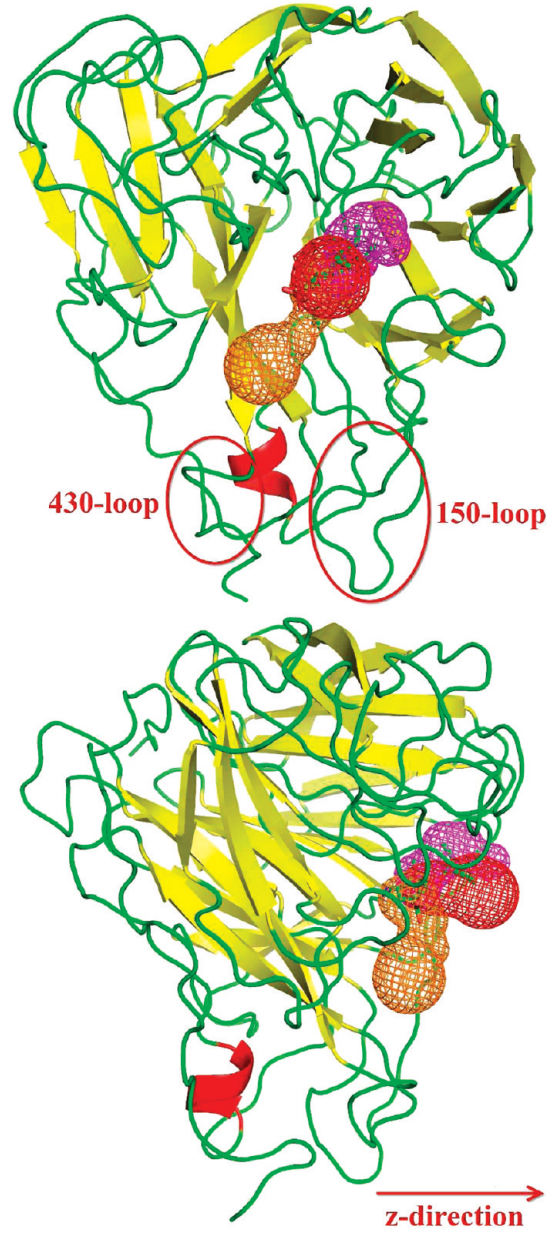


**Figure 2.** Three probable mechanical unbinding paths, obtained by Caver 2.0,[71] for Tamiflu from the drug binding pocket of the WTA/H5N1 neuraminidase. The pathway along the $z$-direction is highlighted in red. The orange mesh refers to the path which goes through loop 430. The angle between the third path (magenta mesh) and $z$-direction is about 30°. The plot has been prepared using software VMD.[91]

of Pymol. Figure 2 shows three possible pathways that the ligand can unbind and escape from the active site. The first pathway (red mesh) is along $z$-direction. This direction goes through a tunnel, which is directed outside the binding pocket and is bounded by residues Asp151, Arg152, Ser246, Glu195, Arg292, Asn347, and Arg371 (see Figure S1 in Supporting Information for more details). The second pathway, denoted by the orange mesh, goes through 430-loop (Figure 2). The third path (magenta mesh) is along the direction which is departed from the $z$-direction by angle of around 30°. If a ligand is pulled along the $z$-direction, then it goes through the widest tunnel (see Supporting Information). Therefore, this is the easiest pathway (lowest rupture force) to pull Tamiflu from the active site of WT H5N1 NA (Figure S2 in Supporting Information). This conclusion

remains valid for pulling other ligands from A/H1N1 neuraminidase (results not shown). Therefore, in this paper the $z$-direction is chosen to pull all of ligands.

**MM-PBSA Method.** The binding free energy is defined by the following equation:

$$\Delta G_{\text{bind}} = G_{\text{complex}} - G_{\text{free-protein}} - G_{\text{free-ligand}} \quad (1)$$

In the MM-PBSA approach one has:

$$\begin{aligned} G &= E_{\text{gas}} + G_{\text{solvation}} - TS \\ G_{\text{solvation}} &= G_{\text{PB}} + G_{\text{sur}} \\ G_{\text{sur}} &= \gamma A + b \end{aligned} \quad (2)$$

The energy in the gas phase $E_{\text{gas}}$ is as follows:

$$E_{\text{gas}} = E_{\text{bond}} + E_{\text{angle}} + E_{\text{tors}} + E_{\text{vdw}} + E_{\text{elec}} \quad (3)$$

Local terms $E_{\text{bond}}$, $E_{\text{angle}}$, and $E_{\text{tors}}$ come from covalent bonds, bending, and torsion interactions. $E_{\text{vdw}}$ and $E_{\text{elec}}$ are the van der Waals and the electrostatic interaction energies, respectively. Total molecular mechanical energies $E_{\text{gas}}$ are calculated by using GROMACS utility with the same force field used in the MD simulations, but no cutoff is used for the evaluation of nonbonded interactions. Within the MM-PBSA approach,[52,53] the free energy is additive (eqs 1−3) containing contributions from different types of interactions. Such a decomposition is useful for understanding the nature of complex systems and is also possible in the more rigorous free energy perturbation approach.[72,73]

$G_{\text{solvation}}$ represents the free energy of solvation and $TS$ is the solute entropic contribution. $G_{\text{solvation}}$ consists of two parts, the polar solvation ($G_{\text{PB}}$) and nonpolar solvation energy ($G_{\text{sur}}$). $G_{\text{PB}}$ arises from the electrostatic potential between solute and solvents and it is determined by using the continuum solvent approximation.[74] The APBS software package[75] was employed for numerical solution of the corresponding linear Poisson−Boltzmann equation. The cubic lattice has a grid spacing of 0.5 Å. The GROMOS radii and charges were used to generate the PQR files. The continuum medium is assumed to have the dielectric constant of water with no salt $\varepsilon = 78.54$ and the solute dielectric constant $\varepsilon = 2$. The surface or nonpolar solvation term $G_{\text{sur}}$ is defined by the solvent-accessible surface area $A$ and two empirical parameters $\gamma = 0.0072$ kcal/(mol Å$^2$) and $b = 0$.[76] Here $A$ was estimated using the Shrake−Rupley numerical approximation[77] implemented in the APBS package.

After equilibration snapshots were taken every 10 ps for estimating the enthalpy. In the MM-PBSA approximation snapshots collected from the MD run for the protein−ligand complex are used for estimating $G_{\text{free-protein}}$ and $G_{\text{free-ligand}}$.

Solute entropy contributions were estimated for the last snapshots taken from MD runs. The structures were minimized with no cutoff for nonbonded interactions by using conjugate gradient and low-memory Broyden−Fletcher−Goldfarb−Shanno method[78] until the maximum force was smaller than $10^{-6}$ kJ/(mol nm). Normal mode analysis was performed by calculating and diagonalizing the mass-weighted Hessian matrix. The frequency of the normal mode was then used to calculate the vibration entropy[79] as given by the following equation:

$$S_{\text{vib}} = -R \ln(1 - e^{-h\nu_0/k_{\text{B}}T}) + \frac{N_{\text{A}} \nu_0 e^{-h\nu_0/k_{\text{B}}T}}{T(1 - e^{-h\nu_0/k_{\text{B}}T})} \quad (4)$$

where $S_{\text{vib}}$ is the vibrational entropy, $h$ Plank's constant, $\nu_0$ the frequency of the normal mode, $k_{\text{B}}$ the Boltzmann constant, $T = 300$ K, and $N_{\text{A}}$ Avogadro's number.

As in the SMD case, for each ligand we have generated four independent trajectories using different random number seeds. The binding free energy is averaged over four runs.

**Measures Used in the Data Analysis.** The mechanical unbinding force which characterizes the binding ability of a ligands to a protein is identified as the maximum force, $F_{\text{max}}$, in the force-time or force-displacement profile. Hydrogen bond is formed if (i) the distance between proton donor (D) and acceptor (A) atoms is less than 3.5 Å and (ii) the D−H−A angle is larger than 145°.

## RESULTS AND DISCUSSIONS

**Validity of SMD Approach.** To check if SMD is suitable for studying binding affinity, we apply it to pull the Tamiflu from pockets of the WT and mutants E119G, N294S, H274Y, and Y252H of A/H5N1 neuraminidase. We choose these systems because their binding free energies are known from prior experimental[25] and theoretical[33] works. The emergence of the H274Y and N294S variants was previously observed in oseltamivir-treated patents with H5N1 virus infection.[80] The Y252H substitution leads to a 10-fold increase in sensitivity of this virus to Tamiflu.[25] Influenza A (H3N2) virus with E119G NA mutations was isolated from patients treated with zanamivir.[81] Since this variant is not resistant to oseltamivir, we used it as a control to test the reliability of SMD in screening out new potent leads.

Typical force-time profiles, obtained for five systems at $v = 0.005$ nm/ps are shown in Figure 3a. Similar results (not shown) were obtained in three other MD runs. Mechanically the E119G complex is the most stable having the highest peak and this result is in accord with the experiments[81] that the E119G variant is not resistant to Tamiflu. We do not address the question about the nature of binding affinity of WT and mutants as it was discussed in detail by Wang and Zheng.[33]

In Figure 3b, the rupture forces are plotted as a function of the binding free energies obtained by the experiments[25] (black squares) and by theory using MM-PBSA method[33] and the force field Amber 99[51] (magenta circles). We obtain a very strong correlation between these two quantities (correlation level $R = 0.99$ and 0.98 for experiments and theory, respectively): the larger the rupture force, the lower is the binding free energy. This result suggests that the SMD method may be used to gain the binding affinity of tamiflu to H5N1 NA and its mutants. Motivated by this observation, we will apply it to study binding of 32 ligands to A/H1N1 neuraminidase. The reliability of SMD approach has been also checked by computation of binding free energies for seven systems using the MM-PBSA method.

**Pulling Ligands from A/H1N1 Neuraminidase.** Figure 4 shows the time (A) and position (B) dependence of force, obtained from one MD run, for Tamiflu, Relenza, peramivir, and NCS141562. For first three ligands, the force reaches the maximum at almost the same time, while the peak of NCS141562 occurs at the longer time scale. Such a behavior

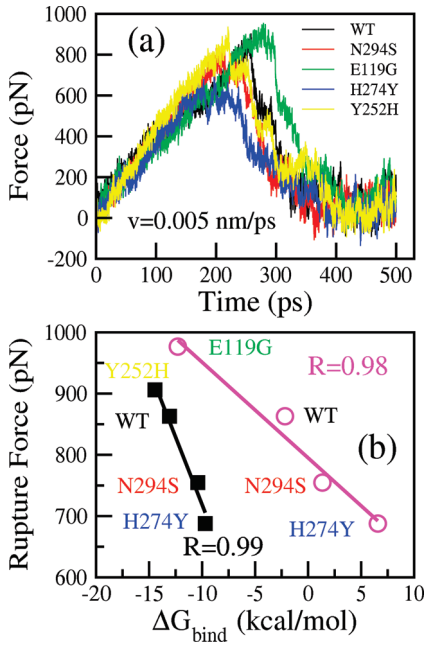


**Figure 3.** (a) Force-time profiles for WT and mutations E119G, H274Y, and N294S of A/H5N1 neuraminidase. (b) Correlation between $F_{max}$ and the binding free energies obtained by experiments (squares). The experimental values of $\Delta G_{bind}$ are estimated from the inhibition constants $K_i$[25] using the formula $\Delta G_{bind} = RT \ln(K_i)$. Here $R = 1.987 \times 10^{-3}$ kcal/mol, $T = 300$ K, and $K_i$ is measured in M. The linear fit $y = 276.6 - 44.2x$ has the correlation level $R = 0.99$. Magenta circles refer to the correlation between the rupture forces and $\Delta G_{bind}$ obtained by Wang and Zeng[33] using the MM-PBSA method and the Amber 99 force field. The correlation level $R = 0.98$ ($y = 794.9 - 15.6x$).

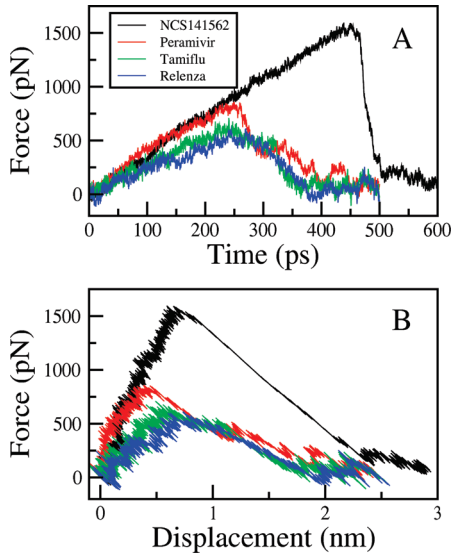


**Figure 4.** (A) Force−time profiles for typical trajectories of Tamiflu, Relenza, peramivir, and NCS141562 in complex with the swine H1N1 neuraminidase. The pulling force is along the $z$-direction. (B) The same as in A but for force−displacement curves.

holds for three other trajectories (Figure S3 in Supporting Information). If one uses the position of the cantilever from its original position, $\Delta z$, as a reaction coordinate, then peaks occur at $\Delta z \approx 0.5-0.7$ nm (Figure 4b). After passing the peak, the force drops rapidly.

Unbinding pathways might be divided into two parts. Before the maximum, the system behaves like a spring as $f$ grows with $\Delta z$ linearly. After the peak the behavior becomes more complicated because of occurrence of a weak peak at large time scales, when a ligand is about to move out from the binding pocket. The minor maximum appears as a result of breaking of HBs between the ligand and residues Asp151 and Arg152. This observation is consistent with the conventional MD result[82] that Asp151 is responsible for flexibility of the 150-loop connecting open and closed conformations in the gating mechanism of H5N1. Since the second peak is very weak, one can neglect it, and then the existence of a single pronounced maximum implies that the mechanical unbinding of ligands follows a two-state scenario. The Relenza shows the weakest resistance to the external force while NCS141562 has the strongest binding with the receptor (Figure 4 and Supporting Information Figure S3).

*Why Tamiflu Is Mechanically More Resistant to A/H5N1 than A/H1N1.* Unbinding of tamiflu from the active site of WT A/H5N1 requires the force $F_{max} \approx 900$ pN (Figure 3), which is higher than $F_{max} \approx 710$ pN for the A/H1N1 case (Figure 4). Thus, the Tamiflu−A/H1N1 NA complex is less stable than the A/H5N1 NA one. This is in accord with prior theoretical works, where the binding free energy, estimated using the same Amber force field,[83] is equal to $\Delta G_{bind} = -15.78 \pm 1.49$ and $-12.8 \pm 0.9$ kcal/mol for H5N1[34] and H1N1,[59] respectively. The MM-PBSA method was employed in ref 34, while authors of ref 59 have implemented the linear interaction energy approximation.

The most notable difference between active sites of H1N1 and H5N1 neuraminidases is that amino acid Y347 is replaced by N347. After the equilibration step of MD simulation, contrary to the H5N1 case, residue N347 moves outward the binding site making its interaction with Tamiflu weaker. This effect presumably comes from reduction of the number of HBs between the ligand and the receptor. To shed light on this problem, we have made two MD runs of 15 ns for Tamiflu−A/H1N1 NA and Tamiflu−A/H5N1 NA complexes. The time dependencies of the HBs number between oseltamivir and the receptors are shown in Figure S4 in Supporting Information. Using these dependencies we obtain the average number of HBs $\approx 3$ and 3.6 for A/H1N1 and A/H5N1, respectively. Thus, the ligand−receptor HB network of the A/H5N1 case is stronger than the A/H1N1 one, leading to differences in binding affinity of Tamiflu to these systems. Using the Caver 2.0[71] program, one can show that the width of the tunnel through which a ligand can moves out is around 3.42 Å for A/H1N1 NA. This value is larger than 2.51 Å for the tunnel of A/H5N1 neuraminidase. Therefore, the mutation Y347N not only reduces the number of HBs between A/H1N1 NA and tamiflu but also widens the binding site. As a result, tamiflu moves out from the active site easier and the corresponding rupture force gets smaller compared to the A/H5N1 case.

*Nature of Mechanical Resistance of Ligands: Hydrogen Bonding versus Electrostatic and van der Waals Interaction.* One can understand the nature of peaks in force−extension profiles by studying the role of HBs, electrostatic, and van der Waals (vdW) interactions. Initially, HBs and nonlocal interactions between a ligand and residues in binding site of NA (especially, Glu119, Asp151, Glu227, Glu277, and Arg371) stabilize a ligand in its position. As the external force grows, the ligand moves out the binding site because its initial configuration becomes unstable. This process is

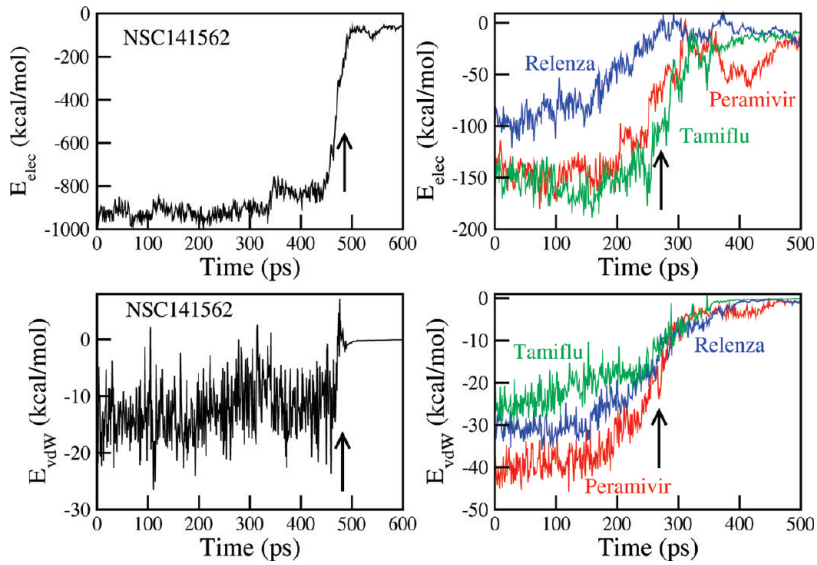


**Figure 5.** Time dependence of the Coulomb and vdW energies for NSC141562, Tamiflu, Relenza, and peramivir. Arrows refer to peak positions in Figure 4a.

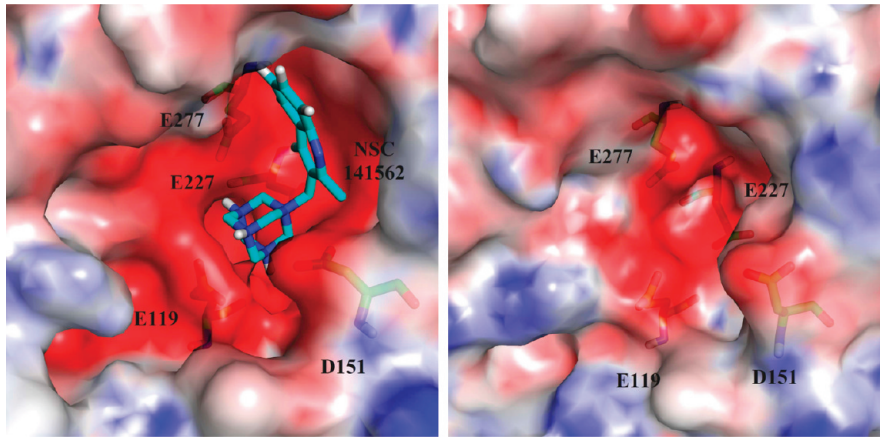


**Figure 6.** Electrostatic potential surfaces of NSC141562 system before (left) and after (right) passing the peak. The plots were prepared by using the PyMOL package. Differences in patterns imply the important role of the Coulomb interactions in ligand binding.

highly nontrivial because of interplay of several kinds of interactions. We will focus on four ligands NCS141562, Tamiflu, peramivir, and Relenza.

As follows from Figure S5 in SI, there are only a few HBs (around 2) between ligand NCS141562 and the active site of A/H1N1 NA. The reason for such a small number of HBs is that these bonds come from interaction with residues Glu119, Asp151, Glu227 and Glu277, carboxyl groups of which are directed toward the ligand (Figure S6 Supporting Information). The existence of a small number of HBs suggests that the nature of the high peak is not entirely associated with HBs. If the number of HBs and pairs of NSC141562 drops abruptly after passing the maximum then such a behavior is not observed for Tamiflu, Relenza, and peramivir (Figure S5 Supporting Information). This is because HBs still survive after the rupture (see, for example, Figure S7 Supporting Information). Therefore, as in the case of NSC141562, the occurrence of peak is not only defined by HBs but also by the Coulomb and vdW interactions.

Although the hydrogen bond number between NCS141562 and the receptor is not large, the electrostatic interactions between residues Glu119, Asp151, Glu227, and Glu277 and three amino groups of this ligand are very strong. This is clearly illustrated in Figure 5 where the time dependence of the electrostatic energy $E_{elec}$ is shown. The force peak occurs at the point where the $E_{elec}$ curve bends. At the maximum in the force−extension profile of NSC141562 the vdW energy $E_{vdW}$ also changes abruptly. Thus, both Coulomb and vdW interactions are responsible for ligand binding but the contribution of the former term dominates (Figure 5). This is also valid for other MD trajectories (Figure S8 Supporting Information). The important role of the Coulomb interaction in mechanical stability of NSC141562 can bee also ascertained by looking at electrostatic potential surfaces before and after the peak (Figure 6). Before rupture, the surface of binding site is predominantly colored by red implying that the ligand mainly interacts with negative charges of NA. Right after the maximum, the substantial change in charge distributions occurs and this plays a key role in formation of the peak in the force-time profile. In short, because of strong Coulomb interactions, the binding free energy of the complex becomes very low making NSC141562 the most prominent to cope with the A/H1N1 virus.

For Tamiflu, Relenza, and peramivir $E_{elec}$ and $E_{vdW}$ curves also bend at peak positions marked by arrows in Figure 5. Therefore, similar to NSC141562 case, both electrostatic and vdW interactions contribute to mechanical stability of these ligands, but again the magnitude of the latter is lower.

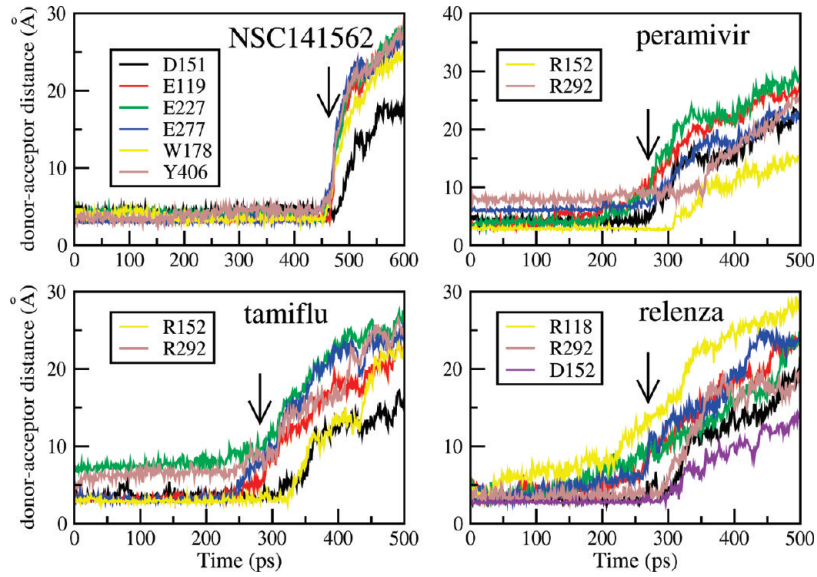


**Figure 7.** Time dependencies of distances between donors and acceptors of ligand and receptors during the unbinding process of Tamiflu, Relenza, peramivir, and NCS141562. Black, red, green, and blue refer to D151, E119, E227, and E277 for all ligands. Arrows refer to peak positions in Figure 4.

**Table 1.** Binding Free Energies of Seven Ligands to A/H1N1 NA Obtained by the MM-PBSA Method[a]

| rank | ligand | $\Delta E_{vdW}$ | $\Delta G_{sur}$ | $\Delta E_{elec}$ | $\Delta G_{PB}$ | $T\Delta S$ | $\Delta G_{bind}$ |
|---|---|---|---|---|---|---|---|
| 1 | 141562 | −6.40 ± 1.09 | −5.16 ± 0.07 | −1003.46 ± 6.94 | 907.92 ± 6.03 | −10.59 ± 0.72 | −96.51 ± 11.35 |
| 2 | 5069 | −33.05 ± 0.94 | −5.00 ± 0.10 | −335.30 ± 14.51 | 307.61 ± 12.76 | −14.75 ± 0.96 | −50.99 ± 4.82 |
| 3 | 46080 | −38.42 ± 2.11 | −5.28 ± 0.13 | −119.17 ± 7.67 | 108.76 ± 6.01 | −15.21 ± 0.37 | −38.90 ± 4.92 |
| 4 | 117079 | −30.29 ± 1.27 | −5.42 ± 0.20 | −118.49 ± 12.16 | 182.08 ± 13.00 | −17.21 ± 0.66 | −34.91 ± 4.95 |
| 5 | peramivir | −37.68 ± 0.84 | −5.00 ± 0.13 | −132.87 ± 3.17 | 139.07 ± 2.83 | −17.14 ± 0.48 | −19.34 ± 0.53 |
| 6 | Tamiflu | −24.89 ± 0.62 | −4.60 ± 0.10 | −155.08 ± 12.23 | 161.49 ± 11.27 | −14.96 ± 0.93 | −8.12 ± 2.62 |
| 7 | Relenza | −30.38 ± 0.30 | −4.95 ± 0.11 | −130.89 ± 6.54 | 142.71 ± 5.59 | −19.03 ± 0.79 | −4.48 ± 3.47 |

[a] Results are averaged over 4 MD trajectories. All values are given in kcal/mol.

Because negative and positive charge groups of Tamiflu and peramivir interact with both negative and positive charges of the receptor in the active site, it is hard for a ligand to find the best position to stabilize all interactions. This is a reason why repulsive interactions between ligands and A/H1N1 NA (for example, the interaction between carbonyl group of peramivir and carboxyl group of Asp151 in Figure S9 Supporting Information) make these complexes less stable compared to NSC141562.

Relenza has 9 charge groups (Figure S10 in Supporting Information) including 3 amino groups (NH), 1 amide (CONH), 1 ether group (C−O−C), 1 carboxyl (COO), and 3 hydroxyls (O−H). Because of this large number of charge groups (Tamiflu, Peramivir, and NSC141562 have 4, 6, and 5 charge groups, respectively) the binding site of NA becomes wider compared to three previous complexes. Repulsive charge−charge interactions are minor but distances between donors and acceptors, which may form HBs, as well as between charges, are large enough (always larger than 2.5 Å, see Figure 7 below), so that the binding ability of Relenza with NA is not high. Besides that, because of enlargement of the pocket surface upon its binding to the receptor, the loss of entropy of the whole complex is higher than that for Tamiflu, peramivir, and NSC141562 (see Table 1 below). This provides the additional contribution to instability of the Relenza−A/H1N1 NA unit (Figure 4).

To obtain a detailed geometrical picture on binding affinity, we use time dependencies of distances between donors and acceptors of ligand and receptor. As follows from Figure 7, the maximum occurs due to the abrupt growth of these distances. Comparing Supporting Information Figure S5 and Figure 7, one can see that monitoring evolution of distances between donors and acceptors of ligand and protein allows for a more detailed description. For NSC141562 unbinding is associated with breaking contacts between the ligand and residues D151, E119, E227, E277, W178, and Y406 of NA. These contacts also contribute to the mechanical resistance of three other ligands (Figure 7). In addition to these six contacts, the interactions with R152 and R292 are important for peramivir and tamiflu, while the stability of relenza depends on positions of not only R292 but also of R118 and D152. Although the number of residuesm which can interact with Relenza is bigger than with other ligands, the mechanical stability of relenza remains low because of gradual time dependence of distances (Figure 7).

Thus, having used the SMD approach, we have shown that in term of ligand binding to A/H1N1 NA the Coulomb interaction is more important than the vdW one. This conclusion is also supported by our results obtained by the MM-PBSA method[52,53] (see below).

**Ranking Binding Affinity of 32 Ligands.** Figure S11 in Supporting Information shows four force-time profiles for the most prominent ligands NSC141562, NSC5069, NSC46080, and NSC117079 (similar results for other compounds are not shown). Using values of $F_{max}$ obtained in four independent MD runs one calculates their average values and error

**Table 2.** Unbinding Force $F_{max}$ obtained by the Gromos 43a1 Force Field for 32 Ligands[a]

| rank | NSC | rupture force (pN) | $E_{bind}$ (kcal/mol)(Dock)[b] | rank (dock)[b] |
|---|---|---|---|---|
| 1 | 141562 | 1769.64 ± 65.34 | −10.04 | 2 |
| 2 | 5069 | 1364.91 ± 40.93 | −8.85 | 6 |
| 3 | 46080 | 1318.45 ± 48.54 | −7.51 | 21 |
| 4 | 117079 | 1296.6 ± 46.22 | −8.46 | 9 |
| 5 | 211332 | 929.21 ± 28.22 | −12.05 | 1 |
| 6 | 131612 | 906.42 ± 20.49 | −8.37 | 10 |
| 7 | 109836 | 861.93 ± 23.68 | −9.47 | 3 |
| 8 | peramivir | 832.21 ± 13.41 | −8.47 | 8 |
| 9 | 90630 | 768.41 ± 20.6 | −8.17 | 13 |
| 10 | 135371 | 730.01 ± 48.08 | −8.36 | 11 |
| 11 | Tamiflu | 707.4 ± 6.41 | −8.15 | 14 |
| 12 | 371688 | 699.85 ± 48.38 | −8.95 | 5 |
| 13 | 164640 | 688.85 ± 27.55 | −8.26 | 12 |
| 14 | 70194 | 688.43 ± 34.98 | −8.07 | 16 |
| 15 | 17245 | 679.44 ± 24.96 | −8.69 | 7 |
| 16 | 327705 | 656.66 ± 14.31 | −8.04 | 17 |
| 17 | 45583 | 646.76 ± 38.58 | −7.69 | 19 |
| 18 | DANA | 640.74 ± 40.64 | −5.1 | 31 |
| 19 | 106920 | 631.56 ± 30.24 | −6.57 | 29 |
| 20 | Relenza | 608.14 ± 37.52 | −7.12 | 26 |
| 21 | 350191 | 602.74 ± 31.61 | −9.56 | 4 |
| 22 | 45576 | 589.59 ± 41.62 | −7.4 | 23 |
| 23 | 16163 | 567.56 ± 26.53 | −6.12 | 30 |
| 24 | 18312 | 561.72 ± 47.71 | −7.46 | 22 |
| 25 | 45582 | 532.36 ± 32.96 | −6.88 | 24 |
| 26 | 37245 | 517.84 ± 22.48 | −7.96 | 18 |
| 27 | 59620 | 494.77 ± 34.69 | −8.07 | 15 |
| 28 | 372294 | 480.55 ± 22.04 | −7.08 | 27 |
| 29 | SA | 469.38 ± 25.85 | −4.82 | 32 |
| 30 | 72254 | 463.51 ± 14.25 | −7.52 | 20 |
| 31 | 148354 | 440.68 ± 14.48 | −7.19 | 25 |
| 32 | 327704 | 434.84 ± 39.13 | −7.27 | 24 |

[a] Results are averaged over 4 pulling trajectories with $v = 0.005$ nm/s. Error bars come from this averaging. [b] Taken from Nguyen et al.[14] for comparison.

bars. The average values of $F_{max}$ (Table 2) were used to rank binding affinity of 32 ligands. The strongest ligand NSC141562 has $F_{max} \approx 1769$ pN, which is about two and half times higher than that for Tamiflu. Together with this champion three ligands NSC5069, NSC46080 and NSC117079 are also mechanically much more stable than other compounds. To pull them out from the active site one needs, at least, to apply a force of ∼1300 pN at pulling speed $v = 0.005$ nm/ps. Therefore, these ligands are expected to have excellent binding affinity and are strongly recommended for clinical trial. Their chemical structures are shown in Figure S12 in Supporting Information. Similar to champion NSC141562, the high binding susceptibility of NSC5069, NSC46080, and NSC117079 comes from strong attractive electrostatic interactions with polar amino acids E119, E227, E277, and D151 in the binding pocket. This is also confirmed by the MM-PBSA results presented below.

Peramivir, Tamiflu, and Relenza are ranked **8**, **11**, and **20**, respectively. Although ranks of Tamiflu and Relenza are different, within error bars, they have compatible values of $F_{max}$ (Figure 8). Our SMD results suggest that eight ligands, including peramivir, can bind with swine A/H1N1 NA better than the commercial drug Tamiflu.

Our predictions are different from those obtained by the docking method[14] (Table 2). This is clearly shown in Figure S13 where the correlation between $F_{max}$ and the binding energy $E_{bind}^{dock}$ is rather low ($R \approx 0.49$). Four most potent leads obtained by the latter method are NSC211332, NSC141562, NCS109836, and NCS350191 which are different from our set of NSC141562, NSC5069, NSC46080, and NSC117079. NCS350191 is ranked **21** in our classification, while it is on the fourth place by the docking method. According to the docking results,[14] in term of binding ability to A/H1N1 NA Relenza (rank **26**) is much worse than Tamiflu (rank **7**). This prediction is at odds with our result that Tamiflu and Relenza would have a compatible binding affinity. Despite several major differences, both the SMD and docking methods predict that NSC141562 belong to the group of four top-hit leads.

We now compare the SMD results with those obtained by the ensemble-based virtual screening for A/H5N1.[12] Our most favorable ligand NSC141562 is ranked **16** for binding to the avian H5N1 neuraminidase. Cheng et al.[12] predicted that NSC109836 is the top-ranked hit **1**, but it is ranked **7** for A/H1N1 (Table. 2). Oseltamivir and Relenza have been shown to be more stable in the H5N1 complex than peramivir, while our results suggest an opposite trend for A/H1N1. Thus, although A/H5N1 and A/H1N1 neuraminidases have high sequence identity their binding properties are markedly different. One of possible reasons lies in the mutation of tyrosine at position 347 by asparagine. However, one has to be cautious in comparison of two systems using results obtained by two different methods.

**Calculation of the Binding Free Energy by MM-PBSA Method.** The SMD results are in excellent agreement with the experimental[25] and MM-PBSA[33] results for WT H5N1 and its mutants (Figure 3). However this conclusion has been drawn from results obtained for only four systems. Therefore it is appealing to perform additional simulations to make sure that 4 top hits revealed by SMD are really better in term of binding affinity than FDA proved drugs tamiflu, relenza and peramivir. For this purpose we have computed $\Delta G_{bind}$ for 7 systems using the MM-PBSA method (see SI).

For each system we have made 4 independent MD runs of 15 ns. The time dependence of the root-mean-square displacement (rmsd) from the initial structures (Figure S14 in SI) shows that systems get equilibrated after 7 ns. Thus snapshots collected every 10 ps for last 8 ns were used for calculating the free energies. The results are shown in Table 1. Clearly, in agreement with the SMD results, 4 top hits are more susceptible to the A/H1N1 NA than tamiflu, relenza and peramivir. For all of ligands studied (Table 1), the electrostatic interaction dominates over the vdW one. Thus the binding affinity is governed not only by HBs but also by the Coulomb interaction.

There is strong correlation ($R = 0.95$) between $\Delta G_{bind}$ obtained by the MM-PBSA and rupture forces for seven compounds (Figure 9). This means that predictive powers of two approaches are comparable. If one uses pulling speed $v = 0.005$ nm/ps for SMD and MD runs of 15 ns for MM-PBSA, then the SMD method is about 30 times faster. This estimate strongly favors the SMD approach as an efficient method for screening out possible leads in the drug design problem.

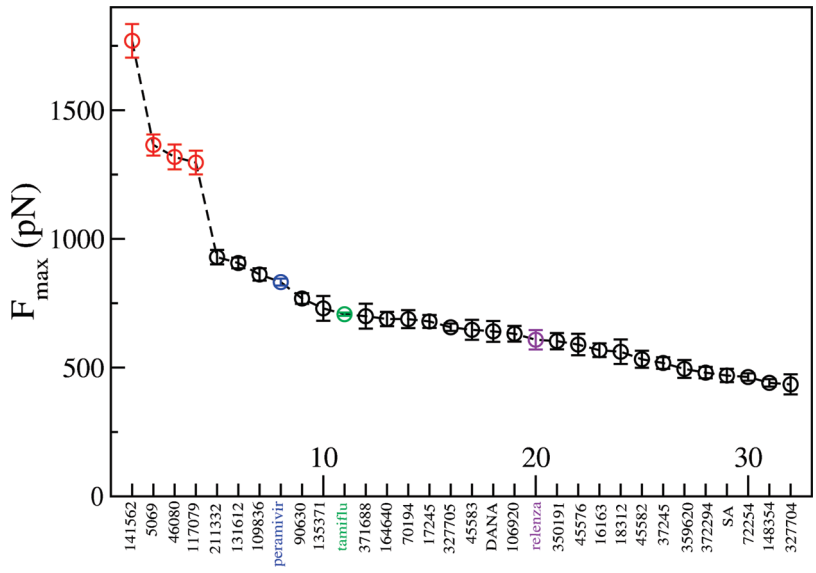


**Figure 8.** Ranking of the binding affinity for 32 ligands using $F_{max}$.

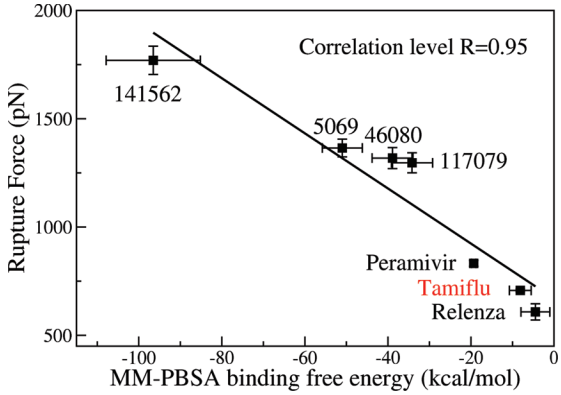


**Figure 9.** Relationship between rupture forces and binding free energies to A/H1N1 NA obtained by the MM-PBSA method for seven ligands. Error bars are from averaging over four MD trajectories. The linear fit is $y = 669.1 - 12.73x$ with correlation level $R = 0.95$.

## DISCUSSION AND CONCLUSION

Having applied the SMD method to study the binding affinity of 32 ligands to the A/H1N1 NA, we have obtained a number of interesting results.

1. We have shown that the SMD can serve as a very promising method for drug design because it reproduces experimental results on binding affinity of Tamiflu to WT and mutants of A/H5N1 neuraminidase. However its reliability needs further investigation.
2. The SMD approach predicts that four top-hit ligands NSC141562, NSC5069, NSC46080, and NSC117079 are potentially more prominent than the existing commercial drugs tamiflu and relenza to cope with the swine 2009 A/H1N1 virus. *This finding is presumably important because both NA enzyme inhibition and X-ray crystallography data suggest that the strategy of designing an inhibitor of NA that binds to its highly conserved active site achieves the desired goal to cope with all influenza NA subtypes, N1−N9, and influenza B viruses.*[84,85] Their high binding affinity comes not only from hydrogen bonding but also from the strong Coulomb interactions with negatively charged residues of the receptor in the active pocket. The fact that these four leads are top-hits is also in the line with our results obtained by the MM-PBSA method and the Gromos 96 43a1 force field.
3. The SMD is shown to be more accurate than the docking approach because the later involves a number of uncontrolled approximations (omission of receptor dynamics and the number of trial positions for ligand is limited). However, one has to bear in mind that the SMD results are sensitive to the choice of pulling direction. So one should be very careful to check what direction to apply the external force to as has been done in this paper using Caver 2.0 program.[71] The conventional SMD may be also used for this purpose.[86,87] Another thing is that the SMD result would depend on the initial position of a ligand in the active pocket. To solve this problem, we first used the docking and then the equilibrium MD run to find the best place to accommodate it.
4. We have shown that the HB network alone does not determine the susceptibility of ligands to A/H1N1 NA. The Coulomb interaction plays a dominant role but the vdW interaction also matters (Figure 5). This is also clearly evident from Figure 7, where some distances between donor and acceptors of ligand and receptors before rupture are larger than the cutoff 3.5 Å for HBs. Their time dependence can be used to identify the nature of the peak in the force-time/displacement profiles. However, using distances between donor and acceptors of ligand and receptors one cannot distinguish contribution of the electrostatic interaction from the vdW one. This problem can be solved either by calculating separate contributions of different interactions to the binding free energy using the MM-PBSA method or by monitoring evolution of $E_{elec}$ and $E_{vdW}$ under mechanical force.
5. We have performed the simulations at the normal density of water of 1 kg/l. Then an interesting question emerges is how does water density influence the unbinding force $F_{max}$. The prior SMD simulations[88] revealed that water molecules fluctuate around the backbone atoms during barrier crossing and weaken interstrand HBs, thereby assisting the mechanical unfolding protein domain I27. This mechanism is also applied to our case where HBs between a ligand and

receptor are attacked by water molecules leading to reduction of $F_{max}$ upon increase of the water density. This is clearly shown in Supporting Information Figure S15, where the unbinding force in the absence of water is about 2-fold higher than that when water is present. Thus $F_{max}$ depends on water density but the general trend shown in Figure 8 remains unchanged.

6. After finishing this work we became aware of the paper of Colizzi et al.[89] who have also used the SMD-derived force profiles to study the binding affinity of six ligands to the unique $\beta$-hydroxyacyl-ACP dehydratase of *Plasmodium falciparum* (*Pf*FabZ) (see also the comment[90] on this paper). Thus, similar to this work our independent study also points to the importance of the SMD approach to the drug design problem. In difference from Colizzi et al., we have shown that the SMD and MM-PBSA have nearly the same predictive power but the former is computationally less expensive.

## ACKNOWLEDGMENT

This work was supported by the Department of Science and Technology of the Ho Chi Minh City, Vietnam and the Ministry of Science and Informatics in Poland (grant No 202-204-234). We thank H.T. Nguyen for very useful discussions.

**Supporting Information Available:** Additional figures including the detailed description of the pulling direction and unbinding process, the number of HBs between ligands and receptors in equilibrium, the correlation between data obtained by SMD and Autodock methods, and the force−displacement profiles in the absence of water. This material is available free of charge via the Internet at http://pubs.acs.org.

## REFERENCES AND NOTES

(1) WHO. A revision of the system of nomenclature for influenza viruses: A WHO memorandum. *Bull. W. H. O.* **1980**, *58*, 585–591.
(2) Murphy, B. R.; Webster, R. G. In *Fields Virology*, 3rd ed.; Lippincott-Raven: Philadelphia, 1996.
(3) Kobasa, D.; Kodihalli, S.; Luo, M.; Castrucci, M. R.; Donatelli, I.; Suzuki, Y.; Suzuki, T.; Kawaoka, Y. Amino acid residues contributing to the substrate specificity of the influenza A virus neuraminidase. *J. Virol.* **1999**, *73*, 6743–6751.
(4) Taisuke, H.; Kawaoka, Y. Pandemic threat posed by avian influenza A viruses. *Clin. Microbiol. Rev. Soc.* **2001**, *14*, 129–149.
(5) WHO. Pandemic (H1N1) 2009, briefing note 4, http://www.who.int/csr/disease/swineflu/notes/h1n1ituation0090724/en/index.html (accessed July 24, 2009).
(6) Ferguson, N. M.; Fraser, C.; Donnelly, C. A.; Ghani, A. C.; Anderson, R. M. Public health risk from the avian H5N1 influenza epidemic. *Science* **2004**, *304*, 968–969.
(7) Le, Q. M.; et al. Avian flu: Isolation of drug-resistant H5N1 virus. *Nature* **2005**, *437*, 1108.
(8) Webster, R. G.; Govorkova, E. A. H5N1 influenza-continuing evolution and spread. *N. Engl. J. Med.* **2006**, *355*, 2174–2177.
(9) *Oseltamivir-resistant 2009 pandemic influenza A (H1N1) virus infection in two summer campers receiving prophylaxis—North Carolina*; Center for Disease Control and Prevention (CDC): United States, 2009; http://www.cdc.gov/mmwr/preview/mmwrhtml/mm5835a1.htm (accessed September 11, 2009).
(10) *Oseltamivir-resistant novel influenza A(H1N1) virus infection in two immunosup-pressed patients—Seattle, Washington*, 2009. MMWR Morb Mortal Wkly Rep. 58: 893−896.
(11) Wkly Epidemiol Rec, Pandemic (H1N1) 2009, briefing note 1 Virus resistant to oseltamivir (tamiflu) identified, http://www.who.int/csr/disease/swineflu/notes/h1n1ntiviralesistance0090708/en/index.html, (accessed July 8, 2009).
(12) Cheng, L. S.; Amaro, R. E.; Xu, D.; Li, W. W.; Arzberger, P. W.; McCammon, J. A. Ensemble-based virtual screening reveals potential novel antiviral compounds for avian influenza neuraminidase. *J. Med. Chem.* **2008**, *51*, 3878–3894.
(13) Sanner, M. F. A. A component-based software environment for visualizing large macromolecular assemblies. *Structure* **2005**, *13*, 447–462.
(14) Nguyen, H. T.; Le, L.; Truong, T. N. Top-hits for A/H1N1 identified by virtual screening using ensemble-based docking. *PLoS Curr.* **2009**, 10.1371/currents.RRN1030.
(15) Li, Y.; Zhou, B.; Wang, R. Rational design of Tamiflu derivatives targeting at the open conformation of neuraminidase subtype 1. *J. Mol. Graphics Modell.* **2009**, *28*, 203–219.
(16) Mihajlovic, M. L.; Mitrasinovic, P. M. Another look at the molecular mechanism of the resistance of H5N1 influenza A virus neuraminidase (NA) to oseltamivir (OTV). *Biophys. Chem.* **2008**, *136*, 152–158.
(17) Garcia-Sosa, A. T.; Sild, S.; Maran, U. Design of multi-binding-site inhibitors, ligand efficiency, and consensus screening of avian influenza h6n1 wild-type neuraminidase and of the oseltamivir-resistant h274y variant. *J. Chem. Inf. Model.* **2008**, *48*, 2074–2080.
(18) Du, Q. S.; Wang, S. Q.; Chou, K. C. Analogue inhibitors by modifying oseltamivir based on the crystal neuraminidase structure for treating drug-resistant H5N1 virus. *Biochem. Biophys. Res. Commun.* **2007**, *362*, 525–531.
(19) Mihajlovic, M. L.; Mitrasinovic, P. M. Applications of the ArgusLab4/AScore protocol in the structure-based binding affinity prediction of various inhibitors of group-1 and group-2 influenza virus neuraminidases (NAs). *Mol. Simul.* **2009**, *35*, 311–324.
(20) Mihajlovic, M. L.; Mitrasinovic, P. M. Some novel insights into the binding of oseltamivir and zanamivir to H5N1 and N9 influenza virus neuraminidases: a homology modeling and flexible docking study. *J. Serb. Chem. Soc.* **2009**, *74*, 1–13.
(21) Mitrasinovic, P. M. On the structure-based design of novel inhibitors of H5N1 influenza A virus neuraminidase (NA). *Biophys. Chem.* **2009**, *140*, 35–38.
(22) Mitrasinovic, P. M. Advances in the structure-based design of the influenza A neuraminidase inhibitors. *Curr. Drug Targets* **2010**, *11*, 315–326.
(23) Morris, G. M.; Goodsell, D. S.; Halliday, R. S.; Huey, R.; Hart, W. E.; Belew, R. K.; Olson, A. J. Automated docking using a Lamarckian genetic algorithm and an empirical binding free energy function. *J. Comput. Chem.* **1998**, *19*, 1639–1662.
(24) Garcia-Sosa, A. T.; Sild, S.; Maran, U. Design of multi-binding-site inhibitors, ligand efficiency, and consensus screening of avian influenza H5N1 wild-type neuraminidase and of the oseltamivir-resistant H274Y variant. *J. Chem. Inf. Model.* **2008**, *48*, 2074–2080.
(25) Collins, P. J.; Haire, L. F.; YP, Y. P. L.; Liu, J. F.; Russell, R. J.; Walker, P. A.; Skehel, J. J.; Martin, S. R.; Hay, A. J.; Gamblin, S. J. Crystal structures of oseltamivir-resistant influenza virus neuraminidase mutants. *Nature* **2008**, *453*, 1258–1261.
(26) Wall, I. D.; Leach, A. R.; Salt, D. W.; Ford, M. G.; Essex, J. W. Binding constants of neuraminidase inhibitors: An investigation of the linear interaction energy method. *J. Med. Chem.* **1999**, *42*, 5142–5152.
(27) Rungrotmongkol, T.; Udommaneethanakit, T.; Malaisree, M.; Nunthaboot, N.; Intharathep, P.; Sompornpisut, P.; Hannongbua, S. How does each substituent functional group of oseltamivir lose its activity against virulent H5N1 influenza mutants. *Biophys. Chem.* **2009**, *145*, 29–36.
(28) Park, J. W.; Jo, W. H. Computational design of novel, high-affinity neuraminidase inhibitors for H5N1 avian influenza virus. *Eur. J. Med. Chem.* **2009**, *45*, 536–541.
(29) Zwanzig, R. W. High-temperature equation of state by a perturbation method. I. Nonpolar gases. *J. Chem. Phys.* **1954**, *22*, 1420–1426.
(30) Bren, U.; Martinek, V.; Florian, J. Free energy simulations of uncatalyzed DNA replication fidelity: Structure and stability of T center dot G and dTTP center dot G terminal DNA mismatches flanked by a single dangling nucleotide. *J. Phys. Chem. B* **2006**, *110*, 10557–10566.
(31) Lee, F. S.; Chu, Z. T.; Bolger, M. B.; Warshel, A. Calculation of antibody antigen interactions-microscopic and semimicroscopic evaluation of the free energies of binding of phosphorylcholine analogs to MCPC603. *Protein Eng.* **1992**, *5*, 215–228.
(32) Bren, U.; Lah, J.; Bren, M.; Martinek, V.; Florian, J. DNA duplex stability: the role of preorganized electrostatics. *J. Phys. Chem. B* **2010**, *114*, 2876–2885.
(33) Wang, N. X.; Zheng, J. J. Computational studies of H5N1 influenza virus resistance to oseltamivir. *Protein Sci.* **2009**, *18*, 707–715.
(34) Masukawa, K. M.; Kollman, P. A.; Kuntz, I. D. Investigation of neuraminidase-substrate recognition using molecular dynamics and free energy calculations. *J. Med. Chem.* **2003**, *46*, 5628–5637.
(35) Bonnet, P.; Bryce, R. A. Molecular dynamics and free energy analysis of neuraminidase ligand interactions. *Protein Sci.* **2004**, *13*, 946–957.

(36) Chachra, R.; Rizzo, R. C. Origins of resistance conferred by the r292k neuraminidase mutation via molecular dynamics and free energy calculations. *J. Chem. Theory Comput.* **2008**, *4*, 1526–1540.
(37) Lawrenz, M.; Baron, R.; McCammon., J. A. Independent-trajectories thermodynamic-integration free-energy changes for biomolecular systems: Determinants of H5N1 avian influenza virus neuraminidase inhibition by peramivir. *J. Chem. Theory Comput.* **2008**, *5*, 1106–1116.
(38) Isralewitz, B.; Baudry, J.; Gullingsrud, J.; Kosztin, D.; Schulten, K. Steered molecular dynamics investigations of protein function. *J. Mol. Graphics Modell.* **2001**, *19*, 13–25.
(39) Isralewitz, B.; Gao, M.; Schulten, K. Steered molecular dynamics and mechanical functions of proteins. *Curr. Opin. Struct. Biol.* **2001**, *11*, 224–230.
(40) Lu, H.; Isralewitz, B.; Krammer, A.; Vogel, V.; Schulten, K. Unfolding of titin immunoglobulin domains by steered molecular dynamics simulation. *Biophys. J.* **1998**, *75*, 662–671.
(41) Isralewitz, B.; Izrailev, S.; Schulten, K. Binding pathway of retinal to bacterioopsin: A prediction by molecular dynamics simulations. *Biophys. J.* **1997**, *73*, 2972–2979.
(42) Grubmuller, H.; Heymann, B.; Tavan, P. Ligand binding: molecular mechanics calculation of the streptavidin−biotin rupture force. *Science* **1996**, *271*, 997–999.
(43) Garter, F.; de Groot, B. L.; Jiang, H.; Grubmuller., H. Ligand-release pathways in the pheromone-binding protein of *Bombyx mori*. *Structure.* **2006**, *14*, 1567–1576.
(44) Xu, Y.; Shen, J.; Luo, X.; Silman, I.; Sussman, J. L.; Chen, K.; Jiang, H. How does huperzine A enter and leave the binding gorge of acetylcholinesterase? Steered molecular dynamics simulations. *J. Am. Chem. Soc.* **2003**, *125*, 11340–11349.
(45) Shen, L.; Shen, J.; Luo, X.; Cheng, F.; Xu, Y.; Chen, K.; Edward, A.; Ding, J.; Jiang, H. Steered molecular dynamics simulation on the binding of NNRTI to HIV-1 RT. *Biophys. J.* **2003**, *84*, 3547–3563.
(46) Park, S.; Khalili-Araghi, F.; Tajkhorshid, E.; Schulten, K. Free energy calculation from steered molecular dynamics simulations using Jarzynski's equality. *J. Chem. Phys.* **2003**, *119*, 3559–3566.
(47) Jensen, M. O.; Park, S.; Tajkhorshid, E.; Schulten, K. Energetics of glycerol conduction through aquaglyceroporin GlpF. *Proc. Natl. Acad. Sci. U.S.A.* **2002**, *99*, 6731–6736.
(48) Zhang, D.; Gullingsrud, J.; McCammon, J. A. Potentials of mean force for acetylcholine unbinding from the alpha7 nicotinic acetylcholine receptor ligand-binding domain. *J. Am. Chem. Soc.* **2006**, *128*, 3019–3026.
(49) Ytreberg, F. M. Absolute FKBP binding affinities obtained via nonequilibrium unbinding simulations. *J. Chem. Phys.* **2009**, *130*, 164906.
(50) Hajjar, E.; Perahia, D.; Debat, H.; Nespoulous, C.; Robert, C. H. Odorant binding and conformational dynamics in the odorant-binding protein. *J. Biol. Chem.* **2006**, *281*, 29929–29937.
(51) Wang, J.; Cieplak, P.; Kollman, P. A. How well does restrained electrostatic potential (RESP) model perform organic and biological molecules. *J. Comput. Chem.* **2000**, *21*, 1049–1074.
(52) Srinivasan, J.; Cheatham, T. E., III; Cieplak, P.; Kollman, P. A.; Case, D. A. Continuum solvent studies of the stability of DNA, RNA, and phosphoramidate-DNA helices. *J. Am. Chem. Soc.* **1998**, *120*, 9401–9409.
(53) Kollman, P. A.; Massova, I.; Reyes, C.; Kuhn, B.; Huo, S.; Chong, L.; Lee, M.; Lee, T.; Duan, Y.; Wang, W.; Donini, O.; Cieplak, P.; Srinivasan, J.; Case, D. A.; Cheatham, T. C., III. Calculating structures and free energies of complex molecules: Combining molecular mechanics and continuum models. *Acc. Chem. Res.* **2000**, *33*, 889–897.
(54) Massova, I.; Kollman, P. A. Computational alanine scanning to probe protein−protein interactions: A novel approach to evaluate binding free energies. *J. Am. Chem. Soc.* **1999**, *121*, 8133–8143.
(55) Ganoth, A.; Friedman, R.; Nachliel, E.; Gutman, M. A molecular dynamics study and free energy analysis of complexes between the Mlc1p protein and two IQ motif peptides. *Biophys. J.* **2006**, *91*, 2436–2450.
(56) Taranta, M.; Bizzarri, A. R.; Cannistraro, S. Modeling the interaction between the N-terminal domain of the tumor suppressor p53 and azurin. *J. Mol. Recognit.* **2008**, *22*, 215–222.
(57) Hess, B.; Kutzner, C.; van der Spoel, D.; Lindahl, E. GROMACS 4: Algorithms for highly efficient, load-balanced, and scalable molecular simulation. *J. Chem. Theory Comput.* **2008**, *4*, 435–447.
(58) Russell, R. J.; Haire, L. F.; Stevens, D. J.; Collins, P. J.; Lin, Y. P.; Blackburn, G. M.; Hay, A. J.; Gamblin, S. J.; Skehel, J. J. The structure of H5N1 avian influenza neuraminidase suggests new opportunities for drug design. *Nature* **2006**, *443*, 45–49.
(59) Rungrotmongkol, T.; Intharathep, P.; Malaisree, M.; Nunthaboot, N.; Kaiyawet, N.; Sompornpisut, P.; Payungporn, S.; Poovorawan, Y.; Hannongbua, S. Susceptibility of antiviral drugs against 2009 influenza A (H1N1) virus. *Biochem. Biophys. Res. Commun.* **2009**, *385*, 390–394.
(60) van Gunsteren, W.; Billeter, S. R.; Eising, A. A.; Hunenberger, P. H.; Kruger, P.; Mark, A. E.; Scott, W. R. P.; Tironi., I. G. *Biomolecular Simulation: The GROMOS96 Manual and User Guide*; Vdf Hochschulverlag AG an der ETH Zurich: Zurich, Switzerland, 1996.
(61) van Aalten, D. M. F.; Bywater, R.; Findlay, J. B. C.; Hendlich, M.; Hooft, R. W. W.; Vriend, G. PRODRG, a program for generating molecular topologies and unique molecular descriptors from coordinates of small molecules. *J. Comput.-Aided. Mol. Des.* **1996**, *10*, 255–262.
(62) Berendsen, H. J. C.; Postma, J. P. M.; van Gunsteren, W. F.; Hermans, J. *Intermolecular Forces*; Reidel, Dordrecht, The Netherlands, 1981.
(63) Hockney, R. W.; Goel, S. P.; Eastwood, J. Quit high resolution computer models of plasma. *J. Comput. Phys.* **1974**, *14*, 148–158.
(64) Hess, B.; Bekker, H.; Berendsen, H. J. C.; Fraaije, J. G. E. M. LINCS: A linear constraint solver for molecular simulations. *J. Comput. Chem.* **1997**, *18*, 1463–1472.
(65) Darden, T.; York, D.; Pedersen, L. Particle mesh Ewald: An $N \log(N)$ method for Ewald sums in large systems. *J. Chem. Phys.* **1993**, *98*, 10089–10092.
(66) Berendsen, H. J. C.; Postma, J. P. M.; van Gunsteren, W. F.; Dinola, A.; Haak, J. R. Molecular dynamics with coupling to an external bath. *J. Chem. Phys.* **1984**, *81*, 3684–3690.
(67) Parrinello, M.; Rahman, A. Polymorphic transitions in single crystals: A new molecular dynamics method. *J. Appl. Phys.* **1981**, *52*, 7182–7190.
(68) Kumar, S.; Li, M. S. Biomolecules under mechanical force. *Phys. Rep.* **2010**, *486*, 1–74.
(69) Kouza, M.; Hu, C. K.; Li, M. S. New force replica exchange method and protein folding pathways probed by force-clamp technique. *J. Chem. Phys.* **2008**, *128*, 045103.
(70) Carrion-Vazquez, M.; Li, H. B.; Lu, H.; Marszalek, P. E.; Oberhauser, A. F.; Fernandez, J. M. The mechanical stability of ubiquitin is linkage dependent. *Nat. Struct. Biol.* **2003**, *10*, 738–743.
(71) Petrek, M.; Otyepka, M.; Banas, P.; Kosinova, P.; Koca1, J.; Damborsky, J. CAVER: A new tool to explore routes from protein clefts, pockets and cavities. *BMC Bioinf.* **2006**, *7*, 316.
(72) Bren, U.; Martinek, V.; Florian, J. Decomposition of the solvation free energies of deoxyribonucleoside triphosphates using the free energy perturbation method. *J. Phys. Chem. B* **2006**, *110*, 12782–12788.
(73) Bren, M.; Florian, J.; Mavri, J.; Bren, U. Do all pieces make a whole? Thiele cumulants and the free energy decomposition. *Theor. Chem. Acc.* **2007**, *117*, 535–540.
(74) Sharp, K. A.; Honig, B. Electrostatic interactions in macromolecules: Theory and applications. *Annu. Rev. Biophys. Biophys. Chem.* **1990**, *19*, 301–332.
(75) Baker, N. A.; Sept, D.; Joseph, S.; Holst, M. J.; McCammon, J. A. Electrostatics of nanosystems: Application to microtubules and the ribosome. *Proc. Natl. Acad. Sci. U.S.A.* **2001**, *98*, 10037–10041.
(76) Sitkoff, D.; Sharp, K. A.; Honig, B. Accurate calculation of hydration free energies using macroscopic solvent models. *J. Phys. Chem.* **1994**, *97*, 1978–1988.
(77) Shrake, A.; Rupley, J. A. Environment and exposure to solvent of protein atoms-lysozyme and insulin. *J. Mol. Biol.* **1973**, *79*, 351–371.
(78) Shanno, D. F. Conditioning of quasi-Newton methods for function minimization. *Math. Comput.* **1970**, *24*, 647–656.
(79) McQuarrie, D. A. *Statistical Thermodynamics*, 2nd ed.; Harper and Row: New York, 1973.
(80) de Jong, M. D.; Thanh, T. T.; Khanh, T. H.; Hien, V. M.; Smith, G. J. D.; Chau, N. V.; Cam, B. V.; Qui, P. T.; Ha, D. Q.; Guan, Y.; Peris, J. M. S.; Hien, T. T.; Farrar, J. Oseltamivir resistance during treatment of influenza A (H5N1) infection. *N. Engl. J. Med.* **2005**, *353*, 2667–2672.
(81) Bright, R. A.; Medina, M. J.; Xu, X. Y.; Perez-Oronoz, G.; Wallis, T. R.; Davis, X. H. M.; Povinelli, L.; Cox, N. J.; Klimov, A. I. Incidence of adamantane resistance among influenza A (H3N2) viruses isolated worldwide from 1994 to 2005: A cause for concern. *Lancet* **2005**, *366*, 1175–1181.
(82) Udommaneethanakit, T.; Rungrotmongkol, T.; U, U. B.; Frecer, V.; Miertus, S. Dynamic behavior of avian influenza A virus neuraminidase subtype H5N1 in complex with oseltamivir, zanamivir, peramivir, and their phosphonate analogues. *J. Chem. Inf. Model.* **2009**, *49*, 2323–2332.
(83) Cornell, W. D.; Ceplak, P.; Bayly, C. I.; Gould, I. R.; Merz, K. M.; Ferguson, D. M.; Spellmeyer, D. C.; Fox, T.; Caldwell, J. W.; Kollman, P. A. A 2nd generation force-filed for the simulation of proteins, nucleic-acids, and organic molecules. *J. Am. Chem. Soc.* **1995**, *117*, 5179–5197.
(84) Govorkova, E. A.; Leneva, I. A.; Goloubeva, O. G.; Bush, K.; Webster, R. G. Comparison of efficacies of RWJ-270201, zanamivir, and oseltamivir against H5N1, H9N2, and other avian influenza viruses. *Antimicrob. Agents Chemother.* **2001**, *45*, 2723–2732.

(85) Roberts, N. A.; Govorkova, E. A. The activity of neuraminidase inhibitor oseltamivir against all subtypes of influenza viruses. In *Global View of the Fight against Influenza*; Mitrasinovic, P. M., Ed; Nova Science Publishers Inc: New York, 2009; pp 93−118.
(86) Liu, X.; Wang, X.; Jiang, H. A steered molecular dynamics method with direction optimization and its applications on ligand molecule dissociation. *J. Biochem. Biophys. Methods* **2008**, *70*, 857–864.
(87) Yang, K.; Liu, X.; Wang, X.; Jiang, H. A steered molecular dynamics method with adaptive direction adjustments. *Biochem. Biophys. Res. Commun.* **2009**, *379*, 494–498.
(88) Lu, H.; Schulten, K. The key event in force-induced unfolding of titin's immunoglobulin domain. *Biophys. J.* **2000**, *79*, 51–65.
(89) Colizzi, F.; Perozzo, R.; Scapozza, L.; Recanatini, M.; Cavalli, A. Single-molecule pulling simulations can discern active from inactive enzyme inhibitors. *J. Am. Chem. Soc.* **2010**, *132*, 7361–7371.
(90) Jorgensen, W. L. Drug discovery pulled from a proteins's embrace. *Nature* **2010**, *466*, 42–43.
(91) Humphrey, W.; Dalke, A.; Schulten, K. VMD−Visual molecular dynamics. *J. Mol. Graphics* **1996**, *14*, 33–38.

CI100346S